Binding of a monoclonal antibody and its Fab fragment to supported phospholipid monolayers measured by total internal reflection fluorescence microscopy

Mary Lee Pisarchick and Nancy L. Thompson
Department of Chemistry, University of North Carolina at Chapel Hill, Chapel Hill, North Carolina 27599-3290 USA

ABSTRACT The association of an anti-dinitrophenyl monoclonal antibody and its Fab fragment with supported phospholipid monolayers composed of a mixture of dipalmitoylphosphatidylcholine and dinitrophenyl-conjugated dipalmitoylphosphatidylethanolamine has been characterized with total internal reflection fluorescence microscopy. The surface densities of bound antibodies were measured as a function of the antibody and Fab solution concentrations, and as a function of the solution concentration of dinitrophenylglycine. The apparent association constant of Fab fragments with surface-associated haptens was ~10-fold lower than the association constant for haptens in solution, and the apparent surface association constant for intact antibodies was only ~10-fold higher than the constant for Fab fragments. Data analysis with simple theoretical models indicated that, at most antibody surface densities, 50–90% of membrane-associated intact antibodies were attached to the surface by two antigen binding sites.

INTRODUCTION

The association of antibodies with cell surfaces is a key molecular event in antibody-mediated immune mechanisms such as phagocytosis, B cell activation, and antibody-dependent cell-mediated cytotoxicity. The relationship of the thermodynamic and kinetic aspects of antibody-membrane association, the translational and rotational mobilities of membrane-bound antibodies, the interactions of membrane-bound antibodies with other cell surface molecules or circulating molecules, and the conformation of membrane-associated antibodies to these immune functions is not yet well understood. The details of the association of antibodies with surfaces are also of importance in the development and application of biosensors and immunodiagnostic devices. This work addresses the relationship between antibody–hapten interactions in solution and on surfaces, and the role of antibody bivalency in surface binding.

One method of investigating the interaction of antibodies with membranelike surfaces is to use phospholipid monolayers or bilayers deposited on planar substrates (Thompson et al., 1988; McConnell et al., 1986). Previous work has demonstrated that hapten-specific monoclonal antibodies bind to supported phospholipid monolayers and bilayers that contain hapten-conjugated phospholipids; that the arrangements and mobilities of the bound antibodies are sensitive functions of the physical and chemical properties of the supported phospholipid films, of the structure and density of the bound antibodies, and of the solution properties; and that immunological cells containing surface receptors for antibodies specifically bind to and metabolically respond to the supported phospholipid films in the presence of hapten-specific antibodies (Timbs and Thompson, 1990; Wright et al., 1988; Tamm, 1988*a*; Subramaniam et al., 1986; Uzgiris, 1986; Hafeman et al., 1981).

A technique for quantitatively characterizing the association of fluorescently-labeled molecules with sites on planar surfaces is total internal reflection fluorescence microscopy (TIRFM; Axelrod et al., 1984). In this technique, the thin evanescent field created by a totally internally reflected excitation source selectively excites surface-bound fluorescent molecules. TIRFM has been used to examine the association of a variety of biochemical ligands with specific surface sites (Poglitsch and Thompson, 1990; Sui et al., 1988; Hlady et al., 1988, 1989; Darst et al., 1988).

TIRFM and supported phospholipid monolayers used in conjunction provide a unique model system amenable to the investigation of protein binding at surfaces. In this work, TIRFM has been applied to the association of a monoclonal anti–dinitrophenyl (DNP) antibody and its Fab fragment with supported phospholipid monolayers containing DNP-conjugated phospholipids. Surface binding curves were obtained as a function of the antibody solution concentrations and as a function of the concentration of competing hapten in solution. In addition, the antibody-hapten association in solution was characterized by tryptophan fluorescence quenching. These data provide a comparison of the association constants of intact antibodies and Fab fragments with haptens in solution and on surfaces, and provide an estimate of the association constant that describes the equilibrium between

intact antibodies bound to the surface by one and two antigen binding sites. This equilibrium is significant because it addresses the biological importance of antibody bivalency, and because it may be related to the translational and rotational mobilities of surface-bound antibodies and, therefore, to potential interactions of surface-bound antibodies with other surface-bound molecules.

THEORETICAL BACKGROUND

Quantitative comparison of association constants for antibodies and haptens undergoing reaction in different states of valency (e.g., Fab fragment vs. intact) and in different geometries (e.g., solution vs. surface) requires assumptions for the binding mechanisms. In this work, the data are analyzed assuming that Fab fragments react with monovalent haptens in solution and on surfaces according to simple bimolecular reactions, and that intact antibodies react with monovalent haptens in solution by two sequential bimolecular reactions.

The association of bivalent anti–hapten antibodies with surfaces that contain an abundance of haptenic sites is more complex. Therefore, three distinct but still simple mechanisms for this interaction have been considered. In model I, a ternary reaction occurs between an antibody and two surface sites. In model II, a bimolecular reaction first occurs between an antibody and a free-surface site, resulting in monovalent surface attachment, and then an isomerization occurs that results in bivalent attachment. In model III, a bimolecular reaction first occurs between an antibody and a free surface site, resulting in monovalent attachment, but then a second bimolecular reaction occurs between the monovalently bound antibody and another free surface site to result in bivalent attachment.

The functional forms of the binding curves for different antibody-hapten binding valencies, geometries, and mechanisms are outlined in this section. These functional forms are used with the experimental data to obtain best-fit parameter values for the equilibrium constants in the different binding mechanisms. The best-fit equilibrium constants that describe the different types of antibody-hapten interactions are then compared. Some of these theoretical expressions have been previously described in similar contexts (e.g., Goldstein et al., 1989; Darst et al., 1988; Erickson et al., 1986; Dower et al., 1981; Perelson and DeLisi, 1980; Reynolds, 1979; Dembo and Goldstein, 1978).

Monovalent antibody fragments and monovalent haptens in solution

Quenching of the ultraviolet fluorescence of anti–DNP antibodies by DNP-conjugated ligands (Pecht and Lancet, 1977; Eisen and Siskind, 1964) or of the visible fluorescence of haptens by specific antibodies (Herron et al., 1986; Lancet and Pecht, 1977) can be used to examine the thermodynamic parameters of antibody-hapten association in solution. In the simplest model, monovalent Fab fragments (M) and monovalent haptens (D) combine to form complexes (MD) with association constant K_s:

$$K_s[M][D] = [MD]. \tag{1}$$

The total concentrations of Fab fragments $[N_M]$ and haptens [T] equal

$$[N_M] = [M] + [MD] \tag{2}$$

$$[T] = [D] + [MD], \tag{3}$$

and the fractions of bound and free Fab fragments are (Eqs. 1 and 2)

$$\frac{[MD]}{[N_M]} = \frac{K_s[D]}{1 + K_s[D]} \tag{4}$$

$$\frac{[M]}{[N_M]} = \frac{1}{1 + K_s[D]}, \tag{5}$$

where the free hapten concentration [D] is (Eqs. 1, 2 and 3)

$$[D] = [K_s([T] - [N_M]) - 1 + \sqrt{\{K_s([T] - [N_M]) - 1\}^2 + 4K_s[T]} \div 2K_s. \tag{6}$$

The fluorescence in the presence of hapten relative to the fluorescence in the absence of hapten is (Eqs. 4 and 5)

$$\frac{F([T])}{F(0)} = \frac{Q_f[M] + Q_b[MD]}{Q_f[N_M]} = \frac{1 - Q_b/Q_f}{1 + K_s[D]} + Q_b/Q_f, \tag{7}$$

where Q_b and Q_f are the fluorescence intensities of bound and free Fab fragments. The best fit of an experimentally determined fluorescence quenching curve $F([T])/F(0)$ to Eqs. 6 and 7 for a known $[N_M]$ yields a measure of the free parameters K_s, Q_b/Q_f, and $F(0)$.

Bivalent antibodies and monovalent haptens in solution

The association of bivalent antibodies (B) and monovalent haptens (D) in solution to form antibodies with one occupied site (BD) and antibodies with two occupied sites (BD_2) is characterized by two equilibrium constants, K_{s1} and K_{s2}, where

$$K_{s1}[B][D] = [BD] \tag{8}$$

$$K_{s2}[BD][D] = [BD_2]. \tag{9}$$

The total antibody and hapten concentrations are

$$[N_B] = [B] + [BD] + [BD_2] \quad (10)$$

$$[T] = [D] + [BD] + 2[BD_2], \quad (11)$$

and the fraction of antibody binding sites that are occupied is (Eqs. 8–10)

$$\frac{½\,[BD] + [BD_2]}{[N_B]} = \frac{K_{s1}[D](1 + 2K_{s2}[D])}{2(1 + K_{s1}[D] + K_{s1}K_{s2}[D]^2)}. \quad (12)$$

If the hapten binding sites are independent, then

$$K_s = ½K_{s1} = 2K_{s2} \quad (13)$$

(Cantor and Schimmel, 1981), Eq. 12 reduces to Eq. 4, Eqs. 8–11 and 13 give the expression in Eq. 6 for the free hapten concentration with $[N_M] = 2[N_B]$, and the process is analogous to that of monovalent antibodies. The normalized fluorescence $F([T])/F([0])$ given by Eqs. 6 and 7 yields a measure of K_s, Q_b/Q_f, and $F(0)$.

Monovalent antibodies and surface-bound haptens

The association of fluorescently-labeled antibodies with surface-bound haptens can be examined by using evanescent illumination, under which the measured fluorescence is in the simplest case proportional to the surface density of bound antibodies (Axelrod et al., 1984). The association of monovalent antibody Fab fragments in solution (M) with sites on a membrane surface (A) to form membrane-bound antibodies (MA) is most simply characterized by a single equilibrium constant K_{m1}, where

$$K_{m1}[M][A] = [MA]. \quad (14)$$

In the experiments described herein, the surface haptens are much smaller than the Fab fragments, and the supported monolayers contain a high molar fraction of hapten-conjugated phospholipid, so that [A] represents the surface density of Fab binding sites but not necessarily of free haptens. The total density of antibody surface sites [S] is

$$[S] = [A] + [MA]. \quad (15)$$

Assuming that the surface does not significantly deplete the solution of antibodies so that the antibody solution concentration [M] equals the applied concentration $[N_M]$ (see below), Eqs. 14 and 15 imply that the surface fluorescence is given by the conventional saturation function

$$\frac{F([N_M])}{F([\infty])} = \frac{[MA]}{[S]} = \frac{K_{m1}[N_M]}{1 + K_{m1}[N_M]}. \quad (16)$$

The best fit of the experimentally measured fluorescence as a function of $[N_M]$ to this functional form yields values for the surface association constant K_{m1} and $F[\infty]$. Of particular interest is the difference between the measured values of the equilibrium constants for haptens in solution (K_s) and membrane-associated haptens (K_{m1}).

Bivalent antibodies and surface-bound haptens

The association of bivalent antibodies with haptenated planar membranes can be investigated by measuring the evanescently excited fluorescence as a function of the solution concentration of free bivalent antibodies. Three simple models that include antibody bivalency are considered. In all of the models, the bivalent antibody solution concentration [B] is assumed to equal the applied concentration $[N_B]$, and the density of antibody surface sites, which does not necessarily equal the hapten density (see above), is denoted by [S].

In model I, the surface association is a single-step mechanism and occurs as a ternary reaction in which antibodies in solution (B) and two free surface sites (A) form surface-bound antibodies (BA_2) with association constant K_{m2}:

$$K_{m2}[B][A]^2 = [BA_2]. \quad (17)$$

The total surface site density equals

$$[S] = [BA_2] + ½[A], \quad (18)$$

and (Eqs. 17 and 18)

$$\frac{F([N_B])}{F(\infty)} = \frac{[BA_2]}{[S]} = \frac{1 + 8K_{m2}[S][N_B] - \sqrt{1 + 16K_{m2}[S][N_B]}}{8K_{m2}[S][N_B]}. \quad (19)$$

Eq. 19 contains two free parameters, $K_{m2}[S]$ and $F(\infty)$; its shape is illustrated in Fig. 1 *a*. The antibody solution concentration $[N_B]$ at which the fluorescence equals one-half the theoretical maximum is $(2K_{m2}[S])^{-1}$.

In model II, the antibody surface association is a two-step process. In the first step, which is bimolecular, an antibody in solution combines with a surface binding site to form an antibody bound by one antigen binding site (BA). In the second step, which is unimolecular, the antibody combines with *an additional free hapten within the surface binding site,* isomerizing to form an antibody bound by two antigen binding sites. This two-step mechanism is characterized by association constants K_{m3} and

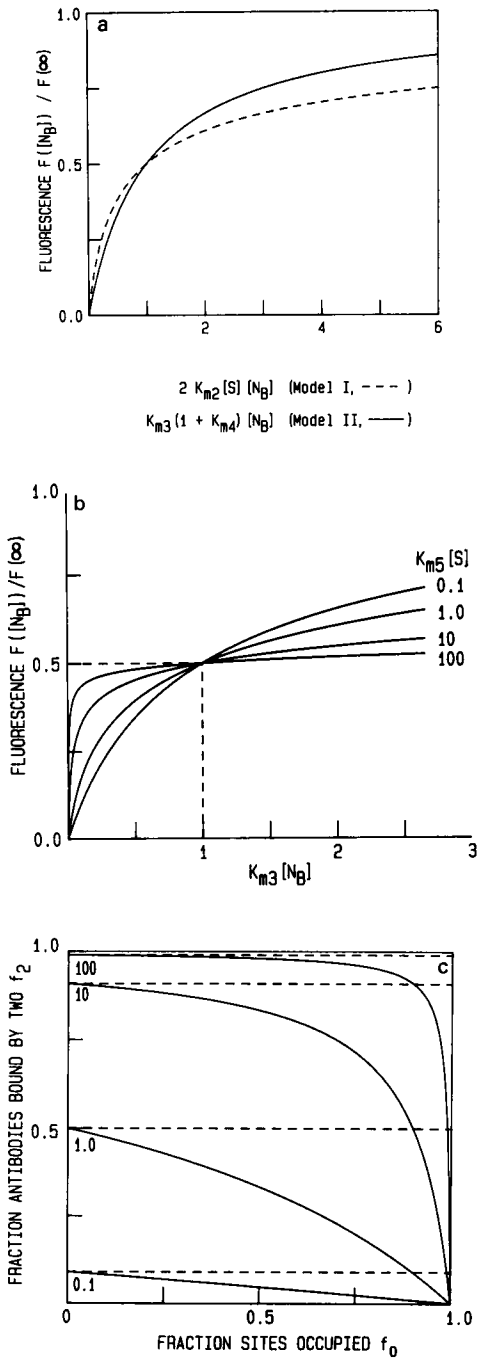

FIGURE 1 Theoretical shape of surface fluorescence as a function of bivalent antibody solution concentration. The fluorescence as a function of the antibody solution concentration monotonically increases: model I, Eq. 19, (*a*, -----); model II, Eq. 23, (*a*, ——); model III, Eq. 26 (*b*). The fraction of bound antibodies that are attached by two sites equals one in model I but depends on the association constants in models II (*c*, -----) and III (*c*, ——); curves are plotted for K_{m4} and $2K_{m5}[S]$ equal to 0.1, 1.0, 10, and 100.

K_{m4} where

$$K_{m3}[B][A] = [BA]; \tag{20}$$

$$K_{m4}[BA] = [BA_2]. \tag{21}$$

The maximum antibody surface density is

$$[S] = [A] + [BA] + [BA_2], \tag{22}$$

and (Eqs. 20–22)

$$\frac{F([N_B])}{F(\infty)} = \frac{[BA] + [BA_2]}{[S]} = \frac{K_{m3}(1 + K_{m4})[N_B]}{1 + K_{m3}(1 + K_{m4})[N_B]}. \tag{23}$$

Eq. 23 has the shape of a conventional saturation curve with two free parameters, $F(\infty)$ and $K_{m3}(1 + K_{m4})$ (Fig. 1 *a*). The apparent association constant ranges from K_{m3} (when $K_{m4} \ll 1$, monovalent binding) to $K_{m3}K_{m4}$ (when $K_{m4} \gg 1$, bivalent binding). The concentration $[N_B]$ at which the fluorescence equals one-half the maximum value is $[K_{m3}(1 + K_{m4})]^{-1}$. Comparison of data obtained for monovalent (Eq. 16) and bivalent (Eq. 23) antibodies provides an estimate of K_{m4} with the assumption that $K_{m1} = K_{m3}$.

In model III, the reaction also occurs in two steps. The first step is identical to that of model II. However, in the second step the antibody undergoes a bimolecular reaction in which an antibody bound to the surface by one antigen binding region combines with *an additional surface binding site* to form an antibody bound by two sites. Eq. 20 and

$$K_{m5}[BA][A] = [BA_2] \tag{24}$$

$$[S] = \tfrac{1}{2}[A] + \tfrac{1}{2}[BA] + [BA_2] \tag{25}$$

imply that

$$\begin{aligned}\frac{F([N_B])}{F(\infty)} &= \frac{[BA] + [BA_2]}{2[S]} \\ &= \Big[1 + 8K_{m5}[S]K_{m3}[N_B] - (K_{m3}[N_B])^2 \\ &\quad + (K_{m3}[N_B] - 1) \\ &\quad \cdot \sqrt{(K_{m3}[N_B] + 1)^2 + 16K_{m5}[S]K_{m3}[N_B]}\Big] \\ &\quad \div 16K_{m5}[S]K_{m3}[N_B].\end{aligned} \tag{26}$$

The fluorescence as a function of the antibody solution concentration contains three free parameters, K_{m3}, $K_{m5}[S]$, and $F(\infty)$ (Fig. 1 *b*). When $K_{m5}[S]$ is small, the process is that of monovalent surface association. Eq. 26 reduces to Eq. 16 with $K_{m1} = K_{m3}$ and $[N_M] = [N_B]$, Eq. 26 reduces to Eq. 23 with $K_{m4} = 0$, and the antibody concentration at which the fluorescence is half maximal is K_{m3}^{-1}. When $K_{m5}[S]$ is large, the experimentally accessible values of $[N_B]$ are much less than K_{m3}^{-1}, Eq. 26 reduces to Eq. 19 with $K_{m2} = K_{m3}K_{m5}$ (multiplied by one-half), and the

antibody concentration at which the fluorescence equals one-half the experimental (not theoretical) maximum is $(2K_{m3}K_{m5}[S])^{-1}$.

In models II and III, the first association constant K_{m3} (Eq. 20) describes the initial antibody-surface association and can be directly compared to the Fab surface association constant K_{m1} (Eq. 14); differences in magnitude suggest that the presence of the second antibody binding site and/or the Fc region influences the initial surface association. The second association constant K_{m4} (Eq. 21) or K_{m5} (Eq. 24) describes the ratio of surface-bound antibodies that are attached to the surface by one or two antigen binding sites:

$$f_2 = \frac{[BA_2]}{[BA] + [BA_2]}. \tag{27}$$

In model II, this ratio is independent of the antibody surface density and equals (Eq. 21)

$$f_2 = \frac{K_{m4}}{1 + K_{m4}}. \tag{28}$$

In model III, the ratio f_2 depends on the fraction of antibody surface sites that are occupied, f_o, where

$$f_o = 1 - \tfrac{1}{2}([A]/[S]), \tag{29}$$

and Eqs. 24, 27, and 29 imply that

$$f_2 = \frac{2K_{m5}[S](1 - f_o)}{1 + 2K_{m5}[S](1 - f_o)}. \tag{30}$$

For most antibody surface densities, very few of the bound antibodies are attached by two sites when $K_{m5}[S]$ is low, and most are bivalently bound when $K_{m5}[S]$ is high. However, for very large antibody solution concentrations and surface coverages, all bound antibodies are attached by only one antigen binding site. The fractions of bound antibodies that are attached by two sites in models II and III are illustrated in Fig. 1 *c*. In model I, $f_2 = 1$.

Inhibition of monovalent antibody surface binding by soluble hapten

Previous work has shown that the binding of anti–DNP antibodies to supported planar membranes containing DNP-conjugated phospholipids is blocked by DNP-glycine (Wright et al., 1988). Experimentally, the evanescently excited fluorescence arising from bound antibodies may be measured as a function of the total concentration of hapten in solution [T] and is relative to the fluorescence in the absence of soluble hapten. If the volume/surface ratio is large enough so that the surface does not deplete the solution of antibodies, Eqs. 1, 2, 14, and 15 imply that

$$\frac{F([T])}{F(0)} = \frac{[MA]}{[MA]_o} = \frac{1 + K_{m1}[N_M]}{1 + K_{m1}[N_M] + K_s[D]}, \tag{31}$$

where $[MA]_o$ is the antibody surface density in the absence of soluble hapten. In the simplest case, the free hapten concentration [D] is approximately equal to the total hapten concentration [T], the best fit of an experimentally measured curve to the form of Eq. 31 with $[D] = [T]$ yields a value for $K_s/(1 + K_{m1}[N_M])$, and a set of curves for different antibody solution concentrations $[N_M]$ provides independent measures of K_s and K_{m1}. If a significant fraction of the haptens are complexed to antibody binding sites, then $[D] \neq [T]$ and the data may be analyzed by fitting the normalized fluorescence $F([T])/F(0)$ to the form of Eq. 31 with [D] given by Eq. 6. The best fit of an experimental curve to this functional form in theory provides values for the free parameters K_s, K_{m1}, $[N_M]$, and $F(0)$ (Fig. 2 *a*).

Inhibition of bivalent antibody surface binding by haptens in solution

The evanescently excited fluorescence arising from bound, intact antibodies is blocked by the presence of high concentrations of solution hapten. Experimentally, the concentration of bound antibodies is measured as a function of the total concentration of hapten in solution and relative to the fluorescence in the absence of soluble hapten. In model I, Eqs. 8–11, 13, 17, and 18 imply that

$$\frac{F([T])}{F(0)} = \frac{[BA_2]}{[BA_2]_o} = \Big[(1 + K_s[D])^2 + 8K_{m2}[S][N_B] - (1 + K_s[D])\sqrt{(1 + K_s[D])^2 + 16K_{m2}[S][N_B]}\Big] \div \Big[1 + 8K_{m2}[S][N_B] - \sqrt{1 + 16K_{m2}[S][N_B]}\Big], \tag{32}$$

where [D] is given by Eq. 6 with $[N_M] = 2[N_B]$. The normalized fluorescence decreases as a function of [T] and depends on the values of K_s, $K_{m2}[S]$, and $[N_B]$ (Fig. 2 *b*).

In model II, antibodies with one antigen binding site bound to a surface hapten and the other to a soluble hapten (BDA) are in the following equilibrium

$$K_s[BA][D] = [BDA], \tag{33}$$

and the total density of surface sites equals

$$[S] = [A] + [BA] + [BDA] + [BA_2]. \tag{34}$$

Eq. 11 is approximately correct for a large volume/surface ratio, and together with Eqs. 8–10, 13, 20, 21, 33

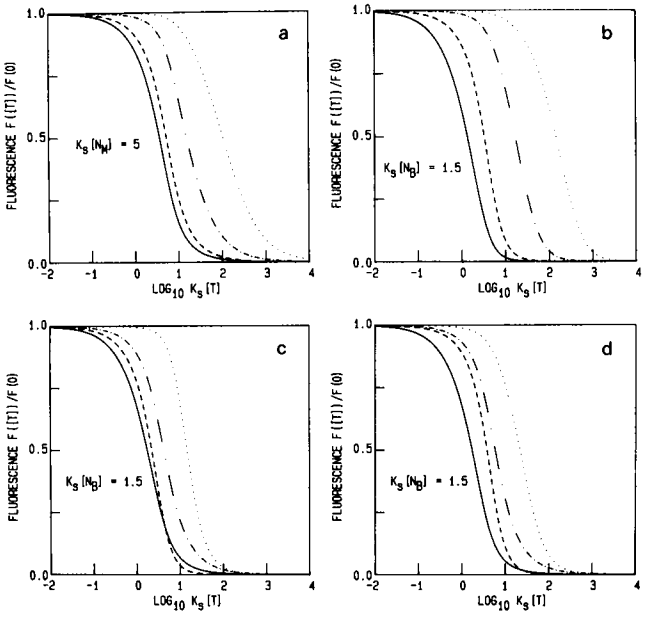

FIGURE 2 Theoretical shape of surface fluorescence as a function of hapten solution concentration. (*a*) The measured fluorescence as a function of the total hapten solution concentration [T] for a given monovalent antibody concentration $[N_M]$ decreases to zero according to Eqs. 31 and 6. For a given solution association constant K_s, the hapten concentration at which the fluorescence is halved increases with the antibody solution concentration $[N_M]$ and with the membrane association constant K_{m1}. Curves are plotted for $K_s[N_M] = 5$ and for $K_{m1}[N_M] = 0.1$ (——), 1.0 (-----), 10 (-·-·-) and 100 (····). The fluorescence for a bivalent antibody solution concentration $[N_B]$ also decreases with the hapten solution concentration [T]: (*b*) model I, Eq. 32, $K_s[N_B] = 1.5$ and $K_{m2}[S][N_B] = 0.01$ (——), 1 (-----), 100 (-·-·-), and 10^4 (····); (*c*) model II, Eq. 35, $K_s[N_B] = 1.5$, and $K_{m3}[N_B] = 0.015$ and $K_{m4} = 1$ (——), $K_{m3}[N_B] = 0.015$ and $K_{m4} = 100$ (-----), $K_{m3}[N_B] = 1.5$ and $K_{m4} = 1$ (-·-·-), $K_{m3}[N_B] = 1.5$ and $K_{m4} = 100$ (····); (*d*) model III, Eq. 37, $K_s[N_B] = 1.5$ and $K_{m3}[N_B] = 0.015$ and $K_{m5}[S] = 1$ (——), $K_{m3}[N_B] = 0.015$ and $K_{m5}[S] = 100$ (-----), $K_{m3}[N_B] = 1.5$ and $K_{m5}[S] = 1$ (-·-·-), $K_{m3}[N_B] = 1.5$ and $K_{m5}[S] = 100$ (····).

and 34 implies that

$$\frac{F([T])}{F(0)} = \frac{[BA] + [BDA] + [BA_2]}{\{[BA] + [BDA] + [BA_2]\}_o} = \left[\frac{1 + K_{m4} + K_s[D]}{1 + K_{m4}}\right] \cdot \left[\frac{1 + (1 + K_{m4})K_{m3}[N_B]}{(1 + K_s[D])^2 + (1 + K_{m4} + K_s[D])K_{m3}[N_B]}\right]. \quad (35)$$

Substituting Eq. 6 with $[N_M] = 2[N_B]$ in Eq. 35 gives an expression for the normalized fluorescence as a function of K_s, K_{m3}, K_{m4}, $[N_B]$, and [T] (Fig. 2 *c*). When $K_{m4} = 0$, Eq. 35 reduces to Eq. 31 with $K_{m1}[N_M] = K_{m3}[N_B]$.

In model III, Eqs. 8–11, 13, 20, 24, 33, and

$$[S] = \tfrac{1}{2}[A] + \tfrac{1}{2}[BA] + \tfrac{1}{2}[BDA] + [BA_2] \quad (36)$$

imply that

$$\frac{F([T])}{F(0)} = \frac{[BA] + [BDA] + [BA_2]}{\{[BA] + [BDA] + [BA_2]\}_o} = \Big[(1 + K_s[D])^2 - (K_{m3}[N_B])^2 + 8K_{m5}[S]K_{m3}[N_B] + (K_{m3}[N_B] - 1 - K_s[D]) \cdot \sqrt{(1 + K_{m3}[N_B] + K_s[D])^2 + 16K_{m5}[S]K_{m3}[N_B]}\Big] \div \Big[1 - (K_{m3}[N_B])^2 + 8K_{m5}[S]K_{m3}[N_B] + (K_{m3}[N_B] - 1) \cdot \sqrt{(1 + K_{m3}[N_B])^2 + 16K_{m5}[S]K_{m3}[N_B]}\Big]. \quad (37)$$

When $K_{m5}[S] = 0$, Eq. 37 reduces to Eq. 31 with $K_{m1}[N_M] = K_{m3}[N_B]$; and when $K_{m5}[S]$ is large and $K_{m3}[N_B] \approx 0$, Eq. 37 reduces to Eq. 32 with $K_{m2} = K_{m3}K_{m5}$. The shape of this function is shown in Fig. 2 *d*.

MATERIALS AND METHODS

Antibodies

Polyclonal murine and sheep IgG (Sigma Chemical Co., St. Louis, MO) and murine IgG Fab (Jackson ImmunoResearch, Inc., West Grove, PA) were obtained commercially. The monoclonal murine IgG1 anti–DNP antibody ANO2 (Balakrishnan et al., 1982*a*) was purified from hybridoma supernatants by affinity chromatography with protein A-sepharose 4B (Sigma Chemical Co.) (Wright et al., 1988; Anglister et al., 1984). Binding and elution buffers were 0.05 M Tris(hydroxymethyl)-aminomethane, 0.01% sodium azide, pH 9.0, and 0.1 M sodium citrate, 0.01% sodium azide, pH 4.5, respectively.

ANO2 Fab fragments were prepared by treating intact ANO2 (1–3 mg/ml) with preactivated (30 min, 37°C) papain (Worthington Diagnostics Div., Freehold, NJ) at a 1:100 wt/wt ratio of papain to ANO2 for 20 h at 37°C in phosphate-buffered saline (PBS; 0.05 M sodium phosphate, 0.15 M sodium chloride, and 0.01% sodium azide, pH 7.4) with 10 mM cysteine and 8 mM ethylenediaminetetraacetate. The digestion was quenched with 20 mM iodoacetamide for 1 h at 0°C. ANO2 Fab fragments were purified from digestion mixtures by affinity chromatography with DNP-conjugated human serum albumin (DNP-HSA, Sigma Chemical Co.) coupled to sepharose 4B. The washing and elution buffers were PBS without and with 0.01 M *N*-2,4-dinitrophenylglycine (DNP-glycine), respectively. DNP-glycine was removed by extensive dialysis against PBS. Intact ANO2 antibodies that were sometimes present in Fab preparations were removed by protein A affinity chromatography.

Fluorescence Labeling

Antibodies were labeled with tetramethylrhodamine isothiocyanate (Molecular Probes, Inc., Junction City, OR) as described (Mishell and Shiigi, 1980) and were purified by Sephadex G50-80 chromatography in PBS followed by DNP-HSA-Sepharose affinity chromatography and extensive dialysis against PBS. Labeled (R-) antibody concentrations and the molar ratios of tetramethylrhodamine to antibody (0.1 to 1.0) were determined spectrophotometrically (Mishell and Shiigi, 1980).

Gel electrophoresis

Analysis of antibodies with SDS-PAGE was carried out according to standard methods (Mishell and Shiigi, 1980). Unlabeled and labeled ANO2 and murine IgG and their Fab fragments ran as appropriate bands in SDS-PAGE under reducing and nonreducing conditions. No unreacted tetramethylrhodamine was observed at the dye front when gels were illuminated with ultraviolet radiation.

Spectrofluorometry

Steady-state fluorescence intensities were measured with a spectrofluorometer (Model 8000C; SLM Instruments, Inc., Urbana, IL). The relative fluorescence yields of different preparations of labeled antibodies were obtained with the excitation wavelength equal to 514 nm, and the emitted fluorescence intensity integrated from 530 to 630 nm. The specificity of labeled and unlabeled intact ANO2 and ANO2 Fab was confirmed and quantified by spectrofluorometrically monitoring the fluorescence quenching by DNP-glycine with excitation and emission wavelengths equal to 280 nm and 340 nm, respectively. Control experiments were carried out with rhodamine-labeled and unlabeled polyclonal murine IgG and IgG Fab fragments. Antibody concentrations were 10–30 μg/ml.

Supported phospholipid monolayers

All water was purified to exceed standards for type I reagent grade water. Dipalmitoylphosphatidylcholine (DPPC; Calbiochem-Behring Corp., La Jolla, CA), dinitrophenylaminocaproyldipalmitoyl phosphatidylethanolamine (DNP-cap-DPPE; Avanti Polar Lipids Inc., Birmingham, AL), and *N*-(7-nitro-2-1,3-benzoxadiazol-4-yl) dipalmitoylphosphatidylethanolamine (NBD-DPPE; Avanti Polar Lipids) were obtained commercially and were judged to be pure by thin layer chromatography. Supported planar membranes were prepared by spreading monolayers of DPPC, DPPC:DNP-cap-DPPE (75:25, mol/mol) or NBD-DPPE: DPPC:DNP-cap-DPPE (2:75:25, mol/mol) at 100 Å^2/molecule on the air/water interface of a Joyce-Loebl Langmuir trough (model 4; Vickers Instruments, Inc., Malden, MA), compressing the monolayers to a surface pressure of 35 dyn/cm at 1–2 Å^2/molecule-min, depositing single monolayers on fused silica substrates (1″ × 1″ × 1 mm, Quartz Scientific Inc., Fairport Harbor, OH) treated with octadecyltrichlorosilane (Aldrich Chemical Co., Milwaukee, WI) by vertical dipping at ~ 5 mm/min (Timbs and Thompson, 1990; Wright et al., 1988; von Tscharner and McConnell, 1981), and transfer to PBS.

Labeled and unlabeled antibodies were prepared for use with supported monolayers by 0.22 μm filtration and sedimentation at 100,000 *g* for 2 h. Supported monolayers containing bound, fluorescently-labeled antibodies were prepared by treating the monolayers with 100 μl of 1 mg/ml sheep IgG in PBS for 5 min to block nonspecific binding sites and then with 200 μl of fluorescently-labeled ANO2 or murine IgG with or without DNP-glycine and in 1 mg/ml sheep IgG/PBS for 10 min.

Fluorescence microscopy

The fluorescence microscope consisted of an argon ion laser (Innova 90-3; Coherent Inc., Palo Alto, CA), an inverted optical microscope (Zeiss IM-35, Eastern Microscope Co., Raleigh, NC), and a single-photon counting photomultiplier (model 31034A; RCA, RCA New Products Div., Lancaster, PA) interfaced to an IBM PC AT computer (IBM Instruments Inc., IBM Corp., Danbury, CT), as previously described (Palmer and Thompson, 1989; Wright et al., 1988). The fluorescence arising from labeled antibodies on supported phospholipid monolayers was measured with TIRFM (Axelrod et al., 1984) with previously described conditions (Poglitsch and Thompson, 1990), except that the laser power was 1 μW. The concentrations of labeled ANO2 that remained in solution after equilibration with haptenated monolayers were measured with epifluorescence microscopy by focusing the laser beam to a small spot (~1 μm^3) in the solution ~50 μm from the monolayer surface (Poglitsch and Thompson, 1990). The lateral mobility of NBD-DPPE in DNP-cap-DPPE/DPPC monolayers was measured with fluorescence pattern photobleaching recovery (Smith and McConnell, 1978) as previously described (Wright et al., 1988) except that the spatial periodicity in the sample plane was 4 μm.

Data analysis

Experimentally determined fluorescence intensities were fit to functional forms using the Gauss-Newton routine in ASYST software (Macmillan Software Co., New York, NY). Fluorescence–photobleaching recovery data were analyzed as previously described (Wright et al., 1988).

Solution association constants were obtained from quenching data by the following iterative procedure, which is a modification of a previously published method (McGuigan and Eisen, 1968): (*a*) the fluorescence intensities of ANO2, $F_a([T])$, and polyclonal IgG, $F_p([T])$, were corrected for dilution, which occurred during addition of DNP-glycine, and normalized to maximum values of one; (*b*) $F_p([T])$ was fit to Eq. 7 with [D] = [T] and with free parameters $(K_s)_p$ and $(Q_b/Q_f)_p$; (*c*) to correct for collisional quenching, $F_a([T])$ was divided by Eq. 7 with $K_s = (K_s)_p$, $Q_b/Q_f = (Q_b/Q_f)_p$, and [D] = [T] (first iteration) or [D] equal to the values obtained in step *e* (subsequent iterations); (*d*) the corrected function $F_A([D])$ was fit to Eq. 7 to yield estimates of K_s and Q_b/Q_f; (*e*) [D] was estimated for each data point as the difference between [T] and the product of $[N_M]$ and the antibody binding site fractional occupancy $[1 - F_A([D])]/[1 - (Q_b/Q_f)]$; (*f*) steps (*c*)–(*e*) were repeated five times and the best-fit values of K_s and Q_b/Q_f for the second through fifth iterations were averaged.

RESULTS AND DISCUSSION

Supported phospholipid monolayers

The dependence of the surface pressure on the density of DPPC monolayers at the air/water interface agreed with previously published results (von Tscharner et al., 1981; Phillips and Chapman, 1968). The presence of high-molar fractions of DNP-cap-DPPE significantly changed the interfacial pressure-area curve (Fig. 3). DNP-cap-DPPE/DPPC monolayers labeled with the fluorescent probe NBD-DPPE appeared uniformly fluorescent within optical resolution. Fluorescence recovery after photobleaching indicated that $\leq$10% of the fluorescent lipids were laterally mobile with an apparent diffusion coefficient $\leq 5 \times 10^{-10}$ cm^2/s.

Solution association constants

The fluorescence of tetramethylrhodamine-labeled and unlabeled ANO2 and ANO2 Fab fragments, excited at 280 nm and detected at 340 nm, was quenched by

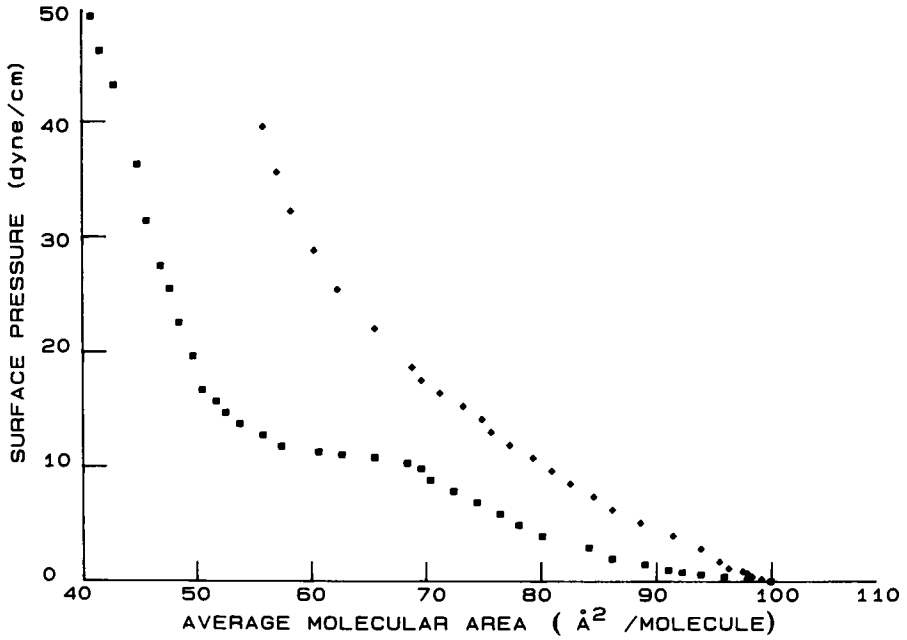

FIGURE 3 Interfacial pressure-area isotherms. Shown is the measured relationship of surface pressure to average molecular area during compression at an air/water interface at 25°C, for DPPC (■) and DNP-cap-DPPE/DPPC (25:75, mol/mol) (♦) monolayers.

DNP-glycine, whereas little fluorescence quenching was observed for unlabeled and labeled murine IgG and its Fab fragment (Fig. 4). This result is consistent with previous reports that DNP-glycine quenches ANO2 fluorescence (Leahy et al., 1988; Anglister et al., 1984). The solution association constants K_s obtained from these data by the iterative procedure described above were equivalent for labeled and unlabeled intact ANO2 and ANO2 Fab (Table 1), and the average value of $K_s = 2.7 \pm 0.2$ μM^{-1} agreed with previous reports (Leahy et al., 1988; Anglister et al., 1984). The fractional quenching at saturation, $1 - (Q_b/Q_f)$, was significantly less for intact ANO2 than for Fab fragments, consistent with the presence of tryptophan residues in the Fc region which are not effectively quenched.

Antibodies on supported monolayers

The evanescently excited fluorescence of supported monolayers treated with 0.1 μM tetramethylrhodamine-labeled antibodies (corrected for the relative fluorescence yields of different antibody preparations) were significantly higher for DNP-cap-DPPE/DPPC monolayers treated with R-ANO2 and R-(ANO2 Fab) than with R-(murine IgG) and R-(murine IgG Fab), were very low for DNP-cap-DPPE/DPPC monolayers treated with R-ANO2 or R-(ANO2 Fab) and high concentrations of DNP-glycine, and were at background levels for DPPC

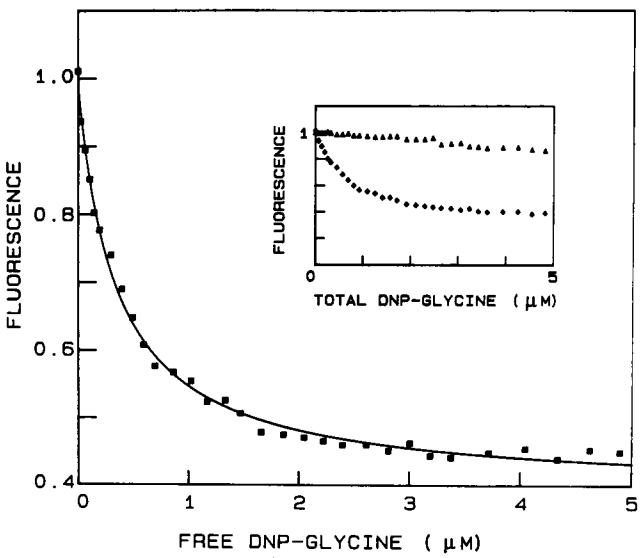

FIGURE 4 Solution equilibrium constants measured by fluorescence quenching. The fluorescence intensity of unlabeled intact ANO2, excited at 280 nm and monitored at 340 nm and corrected for dilution and collisional quenching (see Materials and Methods), is quenched significantly by DNP-glycine (■). The best fit values of K_s and Q_b/Q_f for this curve were 2.9 μM^{-1} and 0.39, respectively. Shown also (*inset*) are the uncorrected fluorescence intensities for unlabeled intact ANO2 (♦) and murine IgG (▲).

TABLE 1. **Solution equilibrium constants of ANO2 antibodies determined by fluorescence quenching**

Antibody	K_s	Q_b/Q_f
	μM^{-1}	
ANO2	2.8 ± 0.2	0.41 ± 0.01
R-ANO2	3.0 ± 0.3	0.47 ± 0.02
ANO2 Fab	2.1 ± 0.1	0.28 ± 0.02
R-(ANO2 Fab)	2.8 ± 0.8	0.19 ± 0.02
Average	2.7 ± 0.2	

Shown are the solution association constants K_s determined from the quenching of ANO2 ultraviolet fluorescence by DNP-glycine. Each value is the mean and standard deviation of the values obtained from three independent ANO2 quenching curves. Each ANO2 quenching curve was corrected for collisional quenching using the average of two curves for the appropriate murine IgG (labeled or unlabeled, intact or Fab).

monolayers treated with R-ANO2 and R-(ANO2 Fab) (data not shown). These results strongly suggest that intact R-ANO2 and R-(ANO2 Fab) specifically bind to DNP-cap-DPPE in DPPC monolayers. DNP-cap-DPPE/DPPC supported monolayers containing bound R-ANO2 and R-(ANO2 Fab) appeared uniformly fluorescent within optical resolution.

Adsorption time for antibodies at supported monolayers

The evanescently excited fluorescence of R-ANO2 and R-(ANO2 Fab) on DNP-cap-DPPE/DPPC monolayers remained constant for times > 10 min and < 1 or 2 h (data not shown). This observation is consistent with previous reports that the density of antibodies bound to other model membrane surfaces is approximately constant after several minutes (Darst et al., 1988; Nygren et al., 1987; Petrossian and Owicki, 1984), suggests that the interaction between solution antibodies and surface haptens rapidly approaches a steady state if not equilibrium, and supports the use of equilibrium expressions in subsequent analysis. Very slow increases in antibody surface densities after very long times have been reported in similar model systems (Darst et al., 1988; Nygren et al., 1987; Uzgirus and Kornberg, 1983) and may also occur for ANO2 antibodies on dinitrophenylated monolayers.

Accuracy of concentration determinations

Previous work has shown that the fluorescence excited by the evanescent field is proportional to the surface density of fluorophores up to at least 14,000 molecules/μm^2 (Lok et al., 1983*a*; Lok et al., 1983*b*), which is well above the estimated antibody surface density at saturation in this work (see below). Solution measurements indicated that saturating amounts (10–100 μM) of DNP-glycine did not affect the intensity of tetramethylrhodamine fluorescence of labeled ANO2 antibodies, in contrast to similar measurements on fluorescein-labeled anti-DNP IgE (Erickson et al., 1987). Thus, the fluorescence measured with TIRFM should be proportional to the antibody surface density.

To determine if the antibody concentrations in solutions adjacent to supported monolayers were equal to the applied concentrations, the fluorescence excited with a laser beam tightly focused in the solution adjacent to antibody-treated supported monolayers was measured. These measurements, calibrated with solutions of known antibody concentrations, indicated that the average solution concentration depletion for applied antibody concentrations was ~ 7% and that very little depletion occurred at higher applied antibody concentrations. This result is consistent with the number of antibodies applied and the estimated antibody surface densities (see below). In addition, an average of ~90% of R-ANO2 and R-(ANO2 Fab) prepared for application to supported monolayers could be readsorbed to DNP-HSA Sepharose 4B and recovered, indicating that a very high fraction of the labeled antibodies retained binding activity for DNP. Thus, the solution concentrations of active antibodies adjacent to the supported monolayers were nearly equal to the applied antibody concentrations.

Fab surface density as a function of Fab solution concentration

The evanescently excited fluorescence of R-(ANO2 Fab) on DNP-cap-DPPE/DPPC monolayers as a function of the Fab solution concentration had the general appearance of a conventional saturation curve, whereas the fluorescence on DPPC monolayers was signficantly lower and was linear with Fab concentration (Fig. 5). The fluorescence on DPPC monolayers was attributed to R-(ANO2 Fab) within the evanescent field but not bound to the surface. The best fit to Eq. 16 of the difference in the measured fluorescence for DNP-cap-DPPE/DPPC and DPPC monolayers, normalized to a maximum value of one, yielded $K_{m1} = 0.31\ \mu M^{-1}$ and $F(\infty) = 1.2$.

The measured association constant K_{m1} for R-(ANO2 Fab) with surface haptens was a factor of nine smaller than the measured association constant K_s for R-(ANO2 Fab) with soluble haptens. Similar differences between solution and surface association constants have been reported for other antibodies (Darst et al., 1988). The discrepancy may reflect the different covalent attachments of the dinitrophenyl moiety to the soluble and surface carrier molecules (glycine and phosphatidylethanolamine). Solution association constants of ANO2 with

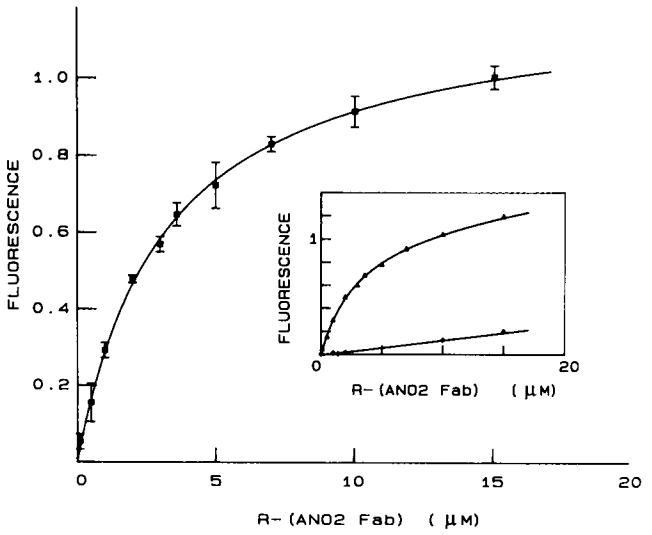

FIGURE 5 R-(ANO2 Fab) binding to DNP-cap-DPPE/DPPC monolayers. The difference (■) of the evanescently excited fluorescence of R-(ANO2 Fab) on DNP-cap-DPPE/DPPC (▲) and DPPC (♦) supported phospholipid monolayers increased with the R-(ANO2 Fab) solution concentration and is compared to the best fit to Eq. 16.

different DNP conjugates can vary within a factor of at least 20 (Leahy et al., 1988).

The lower association constant for surface DNP could also arise from repulsive (including steric) interactions among surface-bound Fabs (Tamm and Bartoldus 1988*b*) or from unfavorable orientations of surface-associated DNP (Stanton et al., 1984; Balakrishnan et al., 1982*b*). For a simple model in which antibody binding sites are equilibrated between accessible (A) and inaccessible (I) states with association constant

$$K_a = [I]/[A], \tag{38}$$

binding and competition curves are given by Eqs. 16 and 31 with K_{m1} replaced by an apparent association constant K^a_{m1}, where

$$K^a_{m1} = \frac{K_{m1}}{1 + K_a} \tag{39}$$

(derivation not shown). If this simple model were to account entirely for the difference between solution and surface haptens, then Eq. 39 implies that $K_a \approx 8$ and that most of the surface haptens are not antibody accessible.

Surface density of intact antibodies as a function of solution concentration

The fluorescence of intact R-ANO2 on DNP-cap-DPPE/DPPC and DPPC supported monolayers as a function of the R-ANO2 solution concentration also reached an apparent saturation (Fig. 6). The apparent association constant of R-ANO2 on DNP-cap-DPPE/DPPC monolayers was ~ 3 μM^{-1}, which is 10-fold higher than that of R-(ANO2 Fab) and similar in value to that measured by conventional assay with separation of bound and free species for ANO2 on fluidlike (~ 8 μM^{-1}; Wright et al., 1988) and solidlike (~ 3 μM^{-1}; Timbs and Thompson, 1990) supported planar membranes.

The binding curve for R-ANO2 was corrected for the fluorescence on DPPC monolayers, normalized to a maximum value of one, and fit to the functional forms of the theoretical expressions for the three different models of bivalent surface attachment. The best fit to Eq. 19 (model I) yielded $2K_{m2}[S] = 1.8\ \mu M^{-1}$ and $F(\infty) = 1.2$, and the best fit to Eq. 23 (model II) yielded $K_{m3}(1 + K_{m4}) = 3.2\ \mu M^{-1}$ and $F(\infty) = 1.0$. The data could not be fit to the functional form of model III (Eq. 26) with K_{m3}, $K_{m5}[S]$, and $F(\infty)$ as free parameters. Therefore, the data were fit to this functional form with $K_{m5}[S]$ fixed (sequentially) at different values and with K_{m3} and $F(\infty)$ as free parameters. Fig. 7 shows the values of K_{m3}, $F(\infty)$, and χ^2 for different values of $K_{m5}[S]$. The data have three regions: when $K_{m5}[S] \leq 0.1$ (monovalent binding), $K_{m3} \simeq 3\ \mu M^{-1}$, $F(\infty) = 1.0$, and χ^2 is low, when $0.1 \leq K_{m5}[S] \leq 100$ (heterogeneous binding), K_{m3} ranges from 3 μM^{-1} to 0.01 μM^{-1}, $F(\infty)$ ranges from 1.0 to 2.4, and χ^2 is high; and when $K_{m5}[S] \geq 100$ (bivalent binding), $2\ K_{m3}K_{m5}[S] \simeq 1.8\ \mu M^{-1}$, K_{m3} is very small, $F(\infty) = 2.4$, and χ^2 is low.

This analysis indicates that either (*a*) the antibodies bind primarily in a monovalent manner, but the association constant of the first antigen binding site is 10-fold larger than that of a single Fab fragment; (*b*) the association constant for a single binding site of the intact antibodies is approximately equal to that of Fab fragments and the constant that describes the equilibrium between antibodies bound by one and two sites is near unity ($K_{m5}[S] \approx 4$); or (*c*) the association constants for the first and second binding events are very low and high, respectively. If K_{m3} equals the measured value of K_{m1}, analysis according to model II implies $K_{m4} = 9$ and according to model III implies $2K_{m5}[S] = 8$, and the calculations in Fig. 1 *c* imply that, at most antibody surface densities, 50–90% of the bound antibodies are linked to the membrane by two sites. This result is consistent with previous efforts to determine the valency of antibody attachment on phospholipid surfaces (Parce et al., 1979).

Maximum antibody surface densities

The ratio r of the fluorescence intensities of DNP-cap-DPPE/DPPC and DPPC monolayers treated with labeled antibodies is, in the absence of nonspecific surface

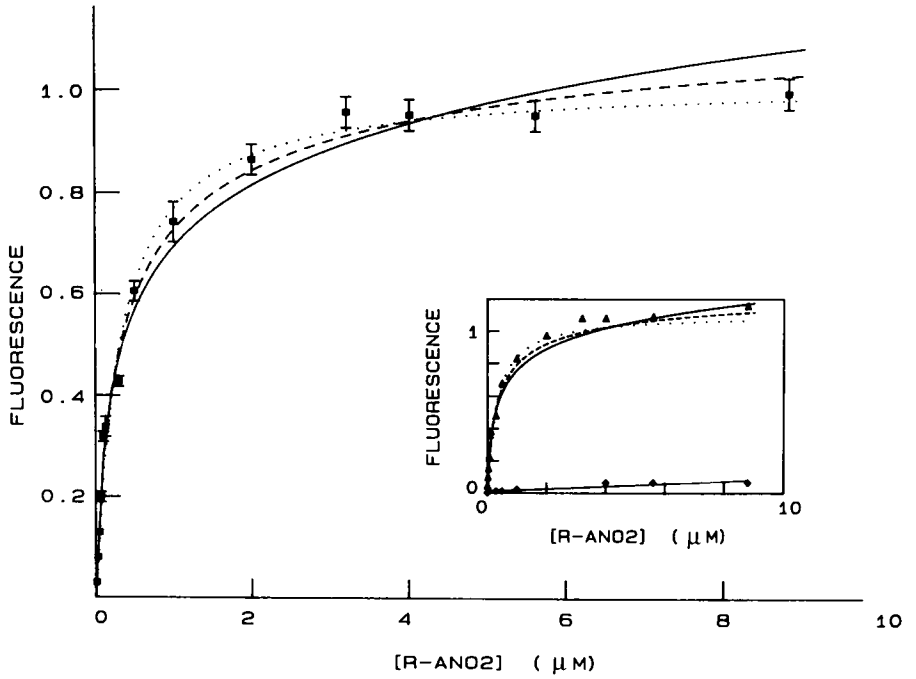

FIGURE 6 Intact R-ANO2 binding to DNP-cap-DPPE/DPPC monolayers. The difference (■) of the evanescently excited fluorescence of R-ANO2 on DNP-cap-DPPE/DPPC (▲) and DPPC (♦) supported phospholipid monolayers increased with the R-ANO2 solution concentration. The data are compared to the best fits to the following theoretical forms: Eq. 19 and Eq. 26 with large (fixed) $K_{m5}[S]$ (-----); Eq. 23 and Eq. 26 with $K_{m5}[S] = 0$ (· · · ·); Eq. 26 with $K_{m5}[S] = 4.0$ (——).

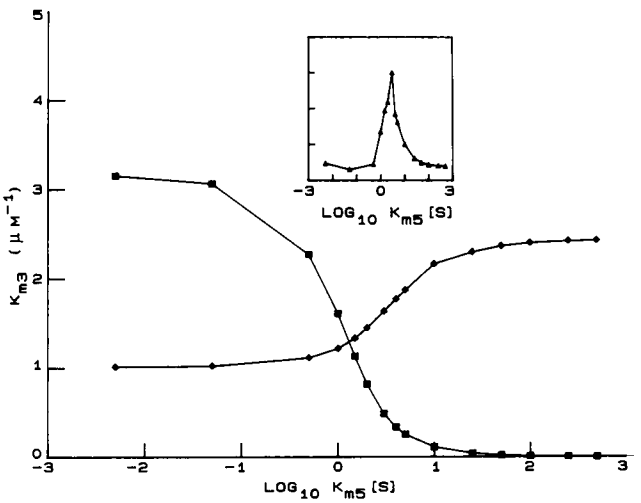

FIGURE 7 Dependence of K_{m3} on $K_{m5}[S]$. The best fits of the data in Fig. 6 to Eq. 26 with fixed, increasing values of $K_{m5}[S]$ produce decreasing values of K_{m3} (■) and increasing values of $F(\infty)$ (♦). Chi-squared (▲, inset) is smaller for lower and higher values of $K_{m5}[S]$.

adsorption,

$$r \approx \frac{[S] + d[N]}{d[N]}, \tag{40}$$

where d is the evanescent field depth ($\approx$ 900 Å) and [N] denotes $[N_M]$ or $[N_B]$. The measured value of r was $\sim$ 12 for [N] = 10 μM, which implies an antibody surface site density [S] $\approx$ 6,000 molecules/μm^2. This value is consistent with antibody size and is in reasonable agreement with previous measurements (Wright et al., 1988; Uzgiris, 1986).

Inhibition of ANO2 Fab and intact ANO2 surface binding by DNP-glycine

The evanescently excited fluorescence of DNP-cap-DPPE/DPPC monolayers treated with R-(ANO2 Fab) or R-ANO2 decreased to the measured fluorescence on DPPC monolayers with increasing concentrations of DNP-glycine in solution and with DNP-glycine half concentrations of $\simeq$ 1 μM. Solution measurements indicated that DNP-glycine at concentrations < 100 μM did not significantly quench the tetramethylrhodamine fluorescence of

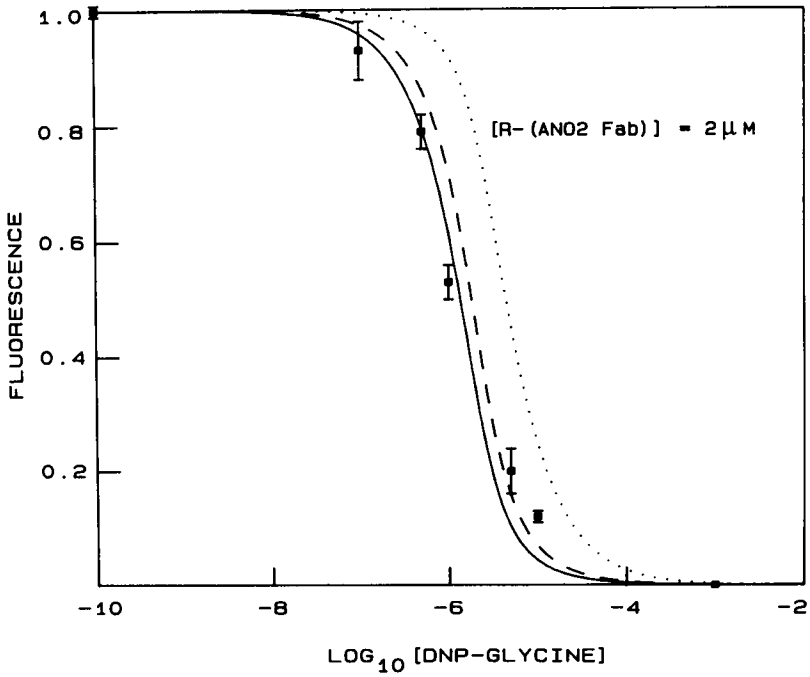

FIGURE 8 Inhibition of R-(ANO2 Fab) binding to DNP-cap-DPPE/DPPC monolayers by DNP-glycine. The evanescently excited fluorescence (■) of 2.0 μM R-(ANO2 Fab) on DNP-cap-DPPE/DPPC supported monolayers decreased with the solution concentration of DNP-glycine. Shown also is Eq. 31 with $K_s = 2.7\ \mu M^{-1}$, $[N_M] = 2.0\ \mu M$, and $K_{m1} = 0$ (——), $0.31\ \mu M^{-1}$ (-----) and $3.1\ \mu M^{-1}$ (····).

labeled polyclonal IgG or ANO2 and, therefore, should-not have affected the proportionality of the measured fluorescence to the antibody surface density.

The fluorescence of R-(ANO2 Fab) on DNP-cap-DPPE/DPPC monolayers as a function of the solution concentration of DNP-glycine was corrected for the fluorescence measured on DPPC monolayers in the absence of DNP-glycine and normalized to a maximum value of one (Fig. 8). The data were fit to the functional form of Eq. 31 with [D] given by Eq. 6. The best fit with K_s and $[N_M]$ set equal to their known values yielded a very low value for K_{m1} (≈ 0). However, the data also agreed well with Eq. 31 when K_{m1} equaled its independently measured value of $0.31\ \mu M^{-1}$ but did not agree well with Eq. 31 when K_{m1} equaled $3\ \mu M^{-1}$. The data, therefore, support but do not independently confirm the measured value of K_{m1}.

The fluorescence of R-ANO2 on DNP-cap-DPPE/DPPC monolayers also decreased with the solution concentration of DNP-glycine. The corrected data were compared with the functional form of Eq. 37 with $K_{m5}[S]$ fixed sequentially as for the direct binding curve (above), K_{m3} fixed at the best-fit values for the given value of $K_{m5}[S]$ shown in Fig. 7, and K_s and $[N_B]$ equal to their experimentally determined values. The analysis showed that the data were consistent with, but could not distinguish among, the full range of pairs of K_{m3} and $K_{m5}[S]$ values (Fig. 9).

Limitations of the theoretical models

Although the simple theoretical models outlined in this work provide adequate data description, several phenomena that may be important in the antibody surface association have not been included. First, the mechanisms simplify possible multistep association reactions between single hapten binding sites and haptens (Pecht, 1982; Pecht and Lancet, 1977). Second, attractive or repulsive interactions among monolayer-bound antibodies or antibody-phospholipid complexes that lead to submicroscopic antibody oligomers (Wright et al., 1988), ordered antibody arrays (Uzgiris and Kornberg, 1983), or steric effects (Tamm and Bartoldus, 1988*b*) could alter apparent antibody surface association constants. Third, submicroscopic coexistent fluid and solid domains in the supported monolayers (McConnell et al., 1984; Seul et al., 1985) in which surface haptens have different antibody accessibilities (Balakrishnan et al., 1982*b*) would result in heterogeneous surface association constants.

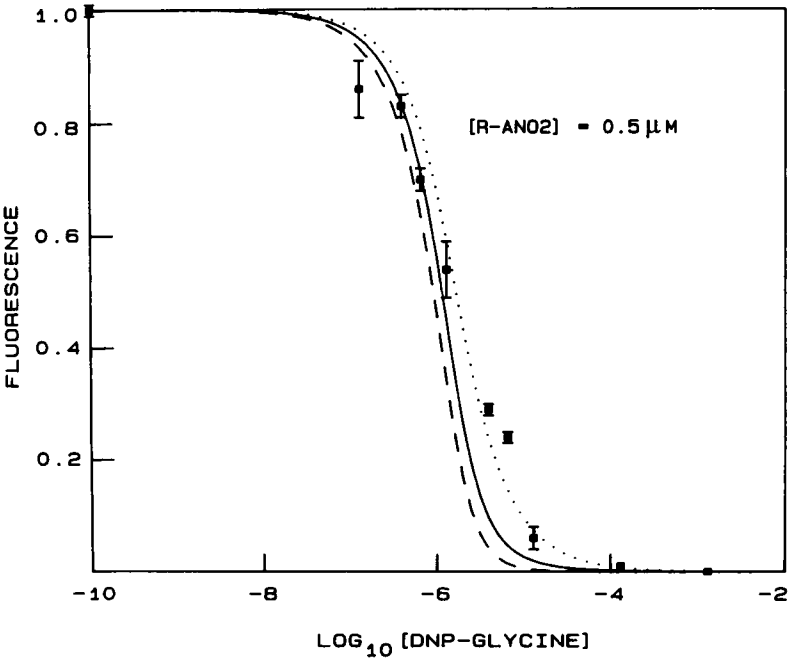

FIGURE 9 Inhibition of intact R-ANO2 binding to DNP-cap-DPPE/DPPC monolayers by DNP-glycine. The evanescently excited fluorescence (■) of 0.5 μM R-ANO2 on DNP-cap-DPPE/DPPC supported monolayers decreased with the solution concentration of DNP-glycine. Shown also is Eq. 37 with $K_s = 2.7\ \mu M^{-1}$ and $K_{m5}[S] = 0$, $K_{m3} = 3.2\ \mu M^{-1}$ (····); $K_{m5}[S] = 4$, $K_{m3} = 0.33\ \mu M^{-1}$ (——); and $K_{m5}[S] = 500$, $K_{m3} = 0.0018\ \mu M^{-1}$ (-----).

SUMMARY

This work has shown that TIRFM can be used to investigate the association of fluorescently-labeled ligands at specific surface sites on supported planar model membranes. One of the key features of the model system is the use of supported membranes, which are unusually resistant to nonspecific protein adsorption. Another advantage of TIRFM for examining surface binding equilibria is that separation of bound and free states is not required, and the technique may be used to measure weak binding constants. The lower limit for measurable association constants is determined primarily by the ratio of bound species to those that are not bound but within the evanescent field and depends on the association constant, the evanescent field depth, the maximum surface site density, and the amount of nonspecific binding (Poglitsch and Thompson, 1990; Thompson et al., 1988). The data in Fig. 5 demonstrate that TIRFM can be used to measure association constants as low as ~0.3 μM^{-1} when the surface site density is ~6,000 molecules/μm^2.

The association constant for the Fab fragment of the anti-DNP monoclonal antibody ANO2 with DNP-cap-DPPE in planar membranes, measured with TIRFM, was ~10-fold smaller than the association constant of ANO2 Fab with DNP-glycine in solution, which suggests that the geometry of Fab-hapten interactions may significantly affect equilibrium parameters. In addition, the apparent association constant for intact ANO2 with planar membranes containing DNP-cap-DPPE, measured with TIRFM, was only ~10-fold higher than that of the ANO2 Fab fragments. This result does not depend on assumed theoretical binding mechanisms and conflicts with the notion that a primary biological function of antibody bivalency is to dramatically increase membrane association constants. In addition, analysis of these data with simple theoretical models suggests that, at equilibrium, only 50–90% of the intact ANO2 bound to planar membranes are attached by two-antigen binding regions.

Future investigations should provide a more thorough understanding of the relationship between antibody and membrane properties to the equilibrium between monovalent and bivalent attachment; and of the relationship between this equilibrium and the lateral (Wright et al., 1988) and rotational (Timbs and Thompson, 1990) mobilities of bound antibodies. The work described herein is also a prerequisite to combining TIRFM with fluorescence photobleaching recovery (Burghardt and Axelrod,

1981) or correlation spectroscopy (Thompson and Axelrod, 1983) to obtain kinetic information.

We thank Harden McConnell of Stanford University for providing ANO2 hybridoma cells. We also thank Arthur Palmer of the Research Institute of the Scripps Clinic, and Claudia Poglitsch, Melanie Timbs, and James Abney of the University of North Carolina for their contributions to biochemical, optical, and conceptual aspects of this work.

Support was provided by National Institutes of Health Grant GM-37145, National Science Foundation Presidential Young Investigator Award DCB-8552986, and a University of North Carolina Junior Faculty Development Award.

Received for publication 19 February 1990 and in final form 2 July 1990.

REFERENCES

Anglister, J., T. Frey, and H. M. McConnell. 1984. Magnetic resonance of a monoclonal anti-spin label antibody. *Biochemistry.* 23:1138–1142.

Axelrod, D., T. P. Burghardt, and N. L. Thompson. 1984. Total internal reflection fluorescence. *Annu. Rev. Biophys. Bioeng.* 13:247–268.

Balakrishnan, K., F. J. Hsu, D. G. Hafeman, and H. M. McConnell. 1982*a*. Monoclonal antibodies to a nitroxide lipid hapten. *Biochim. Biophys. Acta.* 721:30–38.

Balakrishnan, K., S. Q. Mehdi, and H. M. McConnell. 1982*b*. Availability of dinitrophenylated lipid haptens for specific antibody binding depends on the physical properties of host bilayer membranes. *J. Biol. Chem.* 257:6434–6439.

Burghardt, T. P., and D. Axelrod. 1981. Total internal reflection/fluorescence photobleaching recovery study of serum albumin adsorption dynamics. *Biophys. J.* 33:455–468.

Cantor, C. R., and P. R. Schimmel. 1981. Biophysical Chemistry, W. H. Freeman & Co., New York, 852–856.

Darst, S. A., C. R. Robertson, and J. A. Berzofsky. 1988. Adsorption of the protein antigen myoglobin affects the binding of conformation specific monoclonal antibodies. *Biophys. J.* 53:533–539.

Dembo, M., and B. Goldstein. 1978. A thermodynamic model of the binding of flexible bivalent haptens to antibodies. *Immunochemistry.* 15:307–313.

Dower, S. K., C. DeLisi, J. A. Titus, and D. M. Segal. 1981. Mechanism of binding of multivalent immune complexes to Fc receptors. I. Equilibrium binding. *Biochemistry.* 20:6326–6334.

Eisen, H. N., and G. W. Siskind. 1964. Variations in affinities of antibodies during the immune response. *Biochemistry.* 3:996–1008.

Erickson, J. P., P. Kane, B. Goldstein, D. Holowka, and B. Baird. 1986. Cross-linking of IgE receptor complexes at the cell surface: a fluorescence method for studying the binding of monovalent and bivalent haptens to IgE. *Mol. Immunol.* 23:769–781.

Erickson, J., B. Goldstein, D. Holowka, and B. Baird. 1987. The effect of receptor density on the forward rate constant for binding of ligands to cell surface receptors. *Biophys. J.* 52:657–662.

Goldstein, B., R. G. Posner, D. C. Torney, J. Erickson, D. Holowka, and B. Baird. 1989. Competition between solution and cell surface receptors for ligand: dissociation of hapten bound to surface antibody in the presence of solution antibody. *Biophys. J.* 56:955–966.

Hafeman, D. G., V. von Tscharner, and H. M. McConnell. 1981. Specific antibody-dependent interactions between macrophages and lipid haptens in planar lipid monolayers. *Proc. Natl. Acad. Sci. USA.* 78:4552–4556.

Herron, J. N., D. M. Kranz, D. M. Jameson, and E. W. Voss. 1986. Thermodynamic properties of ligand binding by monoclonal anti-fluorescyl antibodies. *Biochemistry.* 25:4602–4609.

Hlady, V., J. Rickel, and J. D. Andrade. 1988/1989. Fluorescence of adsorbed protein layers. II. Adsorption of human lipoproteins studied by total internal reflection intrinsic fluorescence. *Colloids Surf.* 34:171–183.

Lancet, D., and I. Pecht. 1977. Spectroscopic and immunochemical studies with nitrobenzoxadiazolealanine, a fluorescent dinitrophenyl analogue. *Biochemistry.* 16:5150–5157.

Leahy, D. J., G. S. Rule, M. M. Whittaker, and H. M. McConnell. 1988. Sequences of 12 monoclonal anti-dinitrophenyl spin label antibodies for NMR studies. *Proc. Natl. Acad. Sci. USA.* 85:3661–3665.

Lok, B. K., Y. L. Cheng, and C. R. Robertson. 1983*a*. Total internal reflection fluorescence: a technique for examining interactions of macromolecules with solid surfaces. *J. Colloid Interface Sci.* 91:87–103.

Lok, B. K., Y. L. Cheng, and C. R. Robertson. 1983*b*. Protein adsorption on crosslinked polydimethylsiloxane using total internal reflection fluorescence. *J. Colloid Interface Sci.* 91:104–116.

McConnell, H. M., L. Tamm, and R. Weis. 1984. Periodic structures in lipid phase transitions. *Proc. Natl. Sci. USA.* 81:3249–3253.

McConnell, H. M., T. H. Watts, R. M. Weis, and A. A. Brian. 1986. Supported planar membranes in studies of cell-cell recognition in the immune system. *Biochim. Biophys. Acta.* 864:95–106.

McGuigan, J. E., and H. N. Eisen. 1968. Differences in spectral properties and tryptophan content among rabbit anti-2,4-dinitrophenyl antibodies of the γG-immunoglobulin class. *Biochemistry.* 7:1919–1928.

Mishell, B. B., and S. M. Shiigi. 1980. *Selected Methods in Cellular Immunology,* W. H. Freeman and Co., San Francisco, CA. 292–297, 412–436.

Nygren, H., M. Werthen, and M. Stenberg. 1987. Kinetics of antibody binding to solid-phase immobilized antigen. *J. Immunol. Methods.* 101:63–71.

Palmer, A. G., and N. L. Thompson. 1989. High-order fluorescence fluctuation analysis of model protein clusters. *Proc. Natl. Acad. Sci. USA.* 86:6148–6152.

Parce, J. W., M. A. Schwartz, J. C. Owicki, and H. M. McConnell. 1979. Kinetics of antibody association with spin-label haptens on membrane surfaces. *J. Phys. Chem.* 83:3414–3417.

Pecht, I. 1982. Dynamic aspects of antibody function. *In* The Antigens VI. M. Sela, editor. Academic Press Inc., New York. 1–68.

Pecht, I. and D. Lancet. 1977. Kinetics of antibody-hapten interactions. *In* Molecular Biology, Biochemistry and Biophysics 24. I. Pecht and R. Rigler, editors. Springer-Verlag, Heidelberg, 306–338.

Perelson, A., and C. DeLisi. 1980. Receptor clustering on a cell surface. I. Theory of receptor cross-linking by ligands bearing two chemically identical functional groups. *Math. Biosci.* 48:71–110.

Petrossian, A., and J. C. Owicki. 1984. Interactions of antibodies with liposomes bearing fluorescent haptens. *Biochim. Biophys. Acta.* 776:217–227.

Phillips, M. C., and D. Chapman. 1968. Monolayer characteristics of saturated 1,2-diacyl phosphatidylcholines (lecithins) and phosphatidylethanolamines at the air-water interface. *Biochim. Biophys. Acta.* 163:301–313.

Poglitsch, C. L., and N. L. Thompson. 1990. Interaction of antibodies with Fc receptors in substrate-supported planar membranes measured by total internal reflection fluorescence microscopy. *Biochemistry.* 29:248–254.

Reynolds, J. A. 1979. Interaction of divalent antibody with cell surface antigens. *Biochemistry.* 18:264–269.

Seul, M., S. Subramaniam, and H. M. McConnell. 1985. Mono- and bilayers of phospholipids at interfaces: interlayer coupling and phase stability. *J. Phys. Chem.* 89:3592–3595.

Smith, B. A., and H. M. McConnell. 1978. Determination of molecular motion in membranes using periodic pattern photobleaching. *Proc. Natl. Acad. Sci. USA.* 75:2759–2763.

Stanton, S., A. Kantor, A. Petrossian, and J. C. Owicki. 1984. Location and dynamics of a membrane-bound fluorescent hapten: a spectroscopic study. *Biochim. Biophys. Acta.* 776:228–236.

Subramaniam, S., M. Seul, and H. M. McConnell. 1986. Lateral diffusion of specific antibodies bound to lipid monolayers on alkylated substrates. *Proc. Natl. Acad. Sci. USA.* 83:1169–1173.

Sui, S., T. Urumow, and E. Sackmann. 1988. Interaction of insulin receptors with lipid bilayers and specific and nonspecific binding of insulin to supported membranes. *Biochemistry.* 27:7463–7469.

Tamm, L. K. 1988*a*. Lateral diffusion and fluorescence microscope studies on a monoclonal antibody specifically bound to supported phospholipid bilayers. *Biochemistry.* 27:1450–1457.

Tamm, L. K., and I. Bartoldus 1988*b*. Antibody binding to lipid model membranes. The large-ligand effect. *Biochemistry.* 27:7453–7458.

Thompson, N. L., and D. Axelrod. 1983. Immunoglobulin surface binding kinetics measured by total internal reflection with fluorescence correlation spectroscopy. *Biophys. J.* 43:103–114.

Thompson, N. L., A. G. Palmer, L. L. Wright, and P. E. Scarborough. 1988. Fluorescence techniques for supported planar model membranes. *Comm. Mol. Cell. Biophys.* 5:109–131.

Timbs, M. M., and N. L. Thompson. 1990. Slow rotational mobilities of antibodies and lipids associated with substrate-supported phospholipid monolayers as measured by polarized fluorescence photobleaching recovery. *Biophys. J.* 58:413–428.

Uzgiris, E. E. 1986. Supported phospholipid bilayers for two-dimensional protein crystallization. *Biochem. Biophys. Res. Commun.* 134:819–826.

Uzgiris, E. E., and R. D. Kornberg. 1983. Two-dimensional crystallization technique for imaging macromolecules, with application to antigen-antibody-complement complexes. *Nature (Lond.).* 301:125–129.

von Tscharner, V., and H. M. McConnell. 1981. Physical properties of lipid monolayers on alkylated planar glass surfaces. *Biophys. J.* 36:421–427.

Wright, L. L., A. G. Palmer, and N. L. Thompson. 1988. Inhomogeneous translational diffusion of antibodies specifically bound to phospholipid Langmuir-Blodgett films. *Biophys. J.* 54:463–470.